ACS APPLIED MATERIALS & INTERFACES

RESEARCH ARTICLE

www.acsami.org

Resistive-Switching Behavior in Polycrystalline $CaCu_3Ti_4O_{12}$ Nanorods

R. Tararam,[†] E. Joanni,[‡] R. Savu,[§] P. R. Bueno,[*,†] E. Longo,[†] and J. A. Varela[†]

[†]Departamento de Físico-Química, Instituto de Química de Araraquara, Universidade Estadual Paulista (UNESP), Rua Prof. Francisco Degni s/n, 14800-900 Araraquara, São Paulo, Brazil

[‡]Centro de Tecnologia da Informação Renato Archer (CTI), Rod. Dom Pedro I km 143.6, 13069-901 Campinas, São Paulo, Brasil

[§]Centro de Componentes Semicondutores (CCS), Universidade de Campinas (UNICAMP), C.P. 6061, Rua João Pandia Calógeras 90, 13083-870 Campinas, São Paulo, Brazil

ABSTRACT: Highly aligned $CaCu_3Ti_4O_{12}$ nanorod arrays were grown on $Si/SiO_2/Ti/Pt$ substrates by radio-frequency sputtering at a low deposition temperature of 300 °C and room temperature. Structural and morphological studies have shown that the nanostructures have a polycrystalline nature and are oriented perpendicular to the substrate. The high density of grain boundaries in the nanorods is responsible for the nonlinear current behavior observed in these arrays. The current−voltage ($I-V$) characteristics observed in nanorods were attributed to the resistive memory phenomenon. The electrical resistance of microcapacitors composed of $CaCu_3Ti_4O_{12}$ nanorods could be reversibly switched between two stable resistance states by varying the applied electric field. In order to explain this switching mechanism, a model based on the increase/decrease of electrical conduction controlled by grain boundary polarization has been proposed.

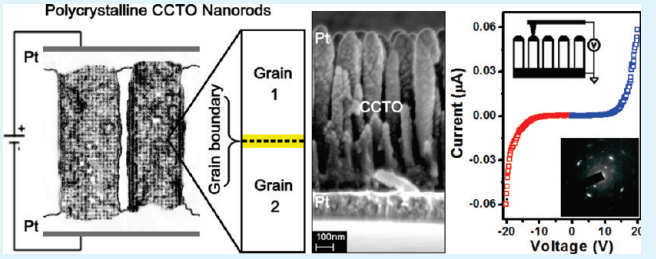

KEYWORDS: CCTO, nanorods, dielectric, nonlinear $I-V$, resistive switching, RF sputtering

1. INTRODUCTION

In the past few years, $CaCu_3Ti_4O_{12}$ (CCTO) ceramics were the subject of intense study, mainly because of their high dielectric permittivity at room temperature, with constant values over a wide temperature range.[1−3] Because of these interesting and unusual dielectric features, CCTO proved to be very interesting from scientific and technological points of view, especially for miniaturization of capacitor-based devices. Moreover, this material exhibits strong nonlinear electrical behavior, even without the addition of dopants, because of the existence of intrinsic potential barriers at the grain boundaries, making it also suitable for application in varistors.[4,5] As a result of these attractive characteristics, CCTO has already been suggested for a variety of applications such as gas sensors,[6] photoluminescent devices,[7] and resistive-switching memory cells.[8]

Even though the majority of results reported so far are related to bulk CCTO samples, thin-film and nanofabrication techniques are expected to yield devices more suitable for practical applications. As a result of this technology-driven search, a variety of chemical and physical techniques have already been employed for obtaining porous and dense CCTO thin films, such as chemical vapor deposition,[9] sol−gel,[10] pulsed laser ablation,[11] and sputtering.[12] On the other hand, rapid advances in nanotechnology led to the fabrication of a large variety of one-dimensional (1D) nanostructures using different deposition strategies in order to explore new effects at the nanoscale level.[13,14] In this context, Joanni et al.[15] recently reported the growth of aligned polycrystalline CCTO nanowires by radio-frequency (RF) sputtering at low substrate temperatures. The method is simple and reproducible, opening the possibility for 1D growth of other oxides.

A large variety of solid-state materials, including perovskites[16] and transition-metal oxides,[17−19] present nonlinear current−voltage ($I-V$) characteristics, with reversible resistance switching induced by applying pulsed voltage at room temperature. This reproducible effect made possible the development of resistive random access memories (ReRAM). These devices offer the advantages of nonvolatility, high switching speed, simple memory cell architecture, low cost, and low energy consumption.[20] The mechanisms responsible for the resistive memory effect in different materials are still the subject of intense debate, with several models being proposed by different researchers. A commonly cited mechanism is based on the formation/rupture of conduction paths formed by the alignment of charged defects. This process depends on the electric field applied and can originate from intrinsic defects in the lattice, impurities, oxygen vacancies, oxygen diffusion, or polarons.[21−25] Other mechanisms proposed are related to the modification of Schottky barriers by charge trapping at the electrode/film interface[26] and to electrochemical migration induced by the applied electric field.[27] For complex oxides, such as CCTO, intensive studies are necessary in order to understand the origin of the resistive-switching behavior.

Received: November 9, 2010
Accepted: December 22, 2010
Published: January 18, 2011

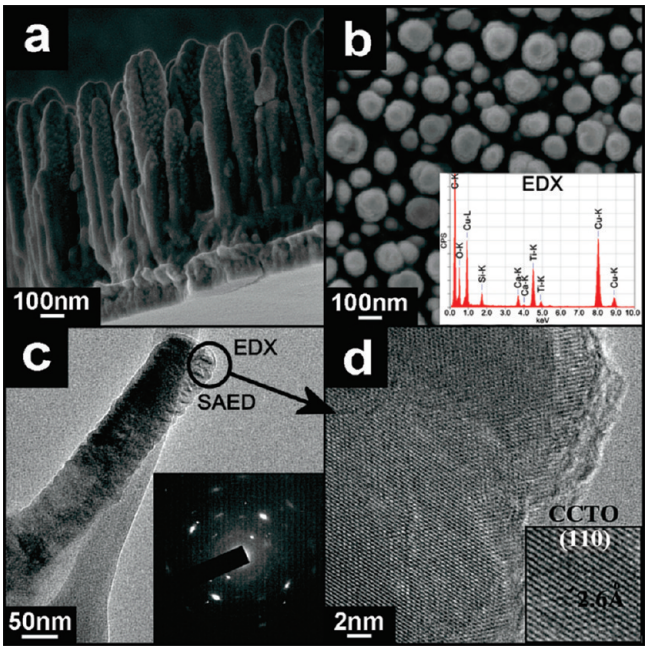

Figure 1. Cross-sectional (a) and surface (b) FE-SEM images showing the morphology of the nanostructured layers obtained at 300 °C for 120 min. TEM (c) and HR-TEM (d) images of a nanorod detached from the same sample. Energy-dispersive X-ray microanalysis (inset in part b) shows compositional information. The SAED pattern (inset in part c) was taken perpendicularly to the rod axis, and the interplanar distance of 2.6 Å was measured to (110).

In this work, we report the fabrication of sputtered polycrystalline CCTO nanorod devices and their characterization, focusing on their potential for application in resistive-switching devices. A model explaining the resistive-switching properties is proposed, based on the increase/decrease of conductivity, Schottky barriers at grain boundaries, and the work of Bueno et al.[28] regarding polaronic transport in CCTO ceramics.

2. EXPERIMENTAL PROCEDURE

2.1. Nanostructural Growth and Device Fabrication. Nanostructured CCTO layers were grown on $Si/SiO_2/Ti/Pt$ substrates by sputtering, using a deposition pressure of 2×10^{-2} mbar of Ar and 150 W RF power. The target−substrate distance was kept constant at 15 cm, and the substrate temperature and deposition time were varied. Different nanorod morphologies and lengths were obtained using two sets of deposition conditions: temperature of 300 °C for 120 min and room temperature for 15 min. For the electrical measurements, top platinum electrodes were deposited by direct-current (dc) sputtering through a shadow mask with circular 172-μm-diameter orifices.

2.2. Characterization. The samples were characterized by X-ray diffraction (XRD; Rigaku Rint 2000), atomic force microscopy (AFM; Nanoscope IIIa, Veeco), field-emission scanning electron microscopy (FE-SEM; Zeiss Supra 35), and transmission electron microscopy (TEM; Jeol JEM 2100). In order to study the resistive properties of the nanorods, $I-V$ measurements were performed at room temperature using a picoammeter (Keithley 6430) in a two-point probe configuration. The positive bias was applied on the top electrode, with the platinum bottom electrode grounded. For measurement of the current in individual nanorods, a Pt−Ir AFM tip (NanoWorld) was used, providing the contact with the platinum electrodes at the nanorod tips. All of the measurements were performed under atmospheric conditions.

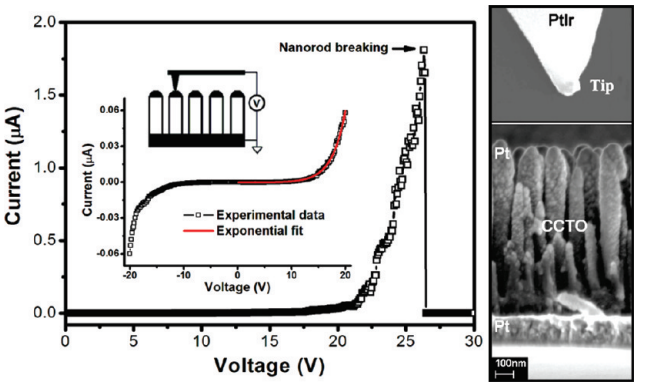

Figure 2. $I-V$ curve showing the behavior of an individual CCTO nanorod. The inset represents a schematic drawing of the configuration adopted for this measurement.

3. RESULTS AND DISCUSSION

3.1. Microstructural and Electrical Characterization. Parts a and b of Figure 1 show the cross-sectional and surface FE-SEM images, respectively, of the sputtered CCTO nanorods deposited at a substrate temperature of 300 °C for 120 min. The aligned nanorods grow perpendicularly to the substrate (Figure 1a), having a coverage density of ∼50% and exhibiting a mean diameter of 80 nm and a length of 900 nm. The platinum contacts deposited at the nanorod tips are clearly visible in the surface image (Figure 1b).

The most important experimental factors for obtaining CCTO nanostructures by sputtering are relatively large target−substrate distances and deposition pressures. The substrate temperature must also be controlled because values above 400 °C lead to the formation of dense films. As previously discussed by Joanni et al.,[15] the mechanism responsible for nanorod formation should involve a balance between the condensation of small polar clusters formed between the target and substrate due to the electric field and the mobility of the deposited material, controlled by the temperature.

The XRD patterns showed no peaks related to the CCTO crystalline phase, indicating an amorphous state for the samples. However, TEM (Figure 1c) and high-resolution TEM (HR-TEM) examination of individual nanorods (Figure 1d) showed that they consist of nanosized crystallites, among which there are noncrystalline areas. The selected-area electron diffraction (SAED) pattern presented in the inset of Figure 1c confirms the polycrystalline nature of the sample. The HR-TEM image (Figure 1d) reveals that the crystals are not randomly assembled, presenting a preferential stacking of the grains along the [110] direction, as confirmed by the measured interplanar distance of ∼2.6 Å in SAED.

A metal−oxide−metal (MOM) configuration was used for studying the electrical behavior of individual nanorods having sputtered platinum as the top electrode. The $I-V$ curve, presented in Figure 2, reveals a strong nonlinear current behavior for these nanorods, similar to the results reported for CCTO bulk ceramics.[4,5] These structures are characterized by a high density of nanoscaled grain boundaries, leading to the pronounced nonlinear resistive behavior observed in the measurements. By sweeping of the voltage (inset in Figure 2) from zero to positive or negative values above a certain voltage, an abrupt increase in the leakage current appears. By this voltage, the low resistance of the film in this state is maintained even after the voltage decreases.

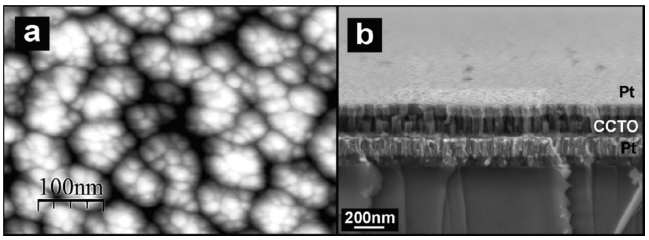

Figure 3. AFM (a) and FE-SEM (b) images showing the surface and cross section, respectively, of the nanostructured film deposited at room temperature for 15 min. The FE-SEM image illustrates the platinum bottom electrode/CCTO nanorods/platinum top electrode microcapacitor configuration.

By sweeping again, the low resistance of the film is recovered to the high resistance in the original state when a reverse voltage is applied. These two stable resistance states are entirely reversible and reproducible depending on the amplitude or polarity of the applied voltage. For these measurements, the current limited is important to ensure reproducibility of measurement and to avoid electrical breakdown and nanorod breaking, observed for currents close to 2 μA (Figure 2). The resistive behavior could possibly be explained by local joule heating,[15,29] but our results indicate that the resistive state can be altered by the electric field and maintained for long time intervals. This behavior is characteristic of the nonvolatile resistive-switching phenomenon, as illustrated by Shen et al.,[8] for sol−gel CCTO thin films. Other oxides showing resistive-switching behavior similar to the one presented in this work were also reported in the literature,[17−19] being considered suitable for ReRAM applications.

Sputtering depositions carried out at room temperature for 15 min resulted also in the anisotropic growth of CCTO. Topographic analyses using the AFM technique (Figure 3a) showed that the nanorods have a high substrate coverage density, being more closely arranged than the structures obtained at 300 °C for 120 min (Figure 1a,b). These highly packed rods allowed deposition of circular top platinum electrodes with 172 μm diameters for building microcapacitors in the MOM configuration (Figure 3b). The sample is composed of aligned nanorods having a length of 130 nm and a diameter of 30 nm, as presented in Figure 3b.

Figure 4a shows the $I-V$ characteristic curve under a voltage sweeping mode for the microcapacitor presented in Figure 3c. An initial electrical forming process is needed to achieve reversible resistive switching.[23,30] This process consists of applying to an electrode's surface a high dc voltage with limited current. The current compliance is needed to avoid hard breakdown of the resistive switching and damage to the device. For a positive bias pulse (+2 V, 1 s) applied to the microcapacitor (SET voltage), a rapid increase in the current can be observed. This maximum value of the current remains even when the voltage decreases.

Furthermore, in the $I-V$ curve, it is observed that the current increases when the voltage rises from zero to positive values. This behavior is characteristic of a nonvolatile low resistance state (ON state). During the SET process, high electric fields promote the alignment of charged defects, presumably along the grain boundaries, which serve as conduction paths. The device stays in the ON state until the negative bias pulse (−2 V, 1 s) is applied during the RESET process, when the device switches back to the high resistance state (OFF state). Besides, the $I-V$ curve shows that when the voltage rises from zero to a positive voltage, the current is low in the OFF state until V_{SET}. Thus, after the

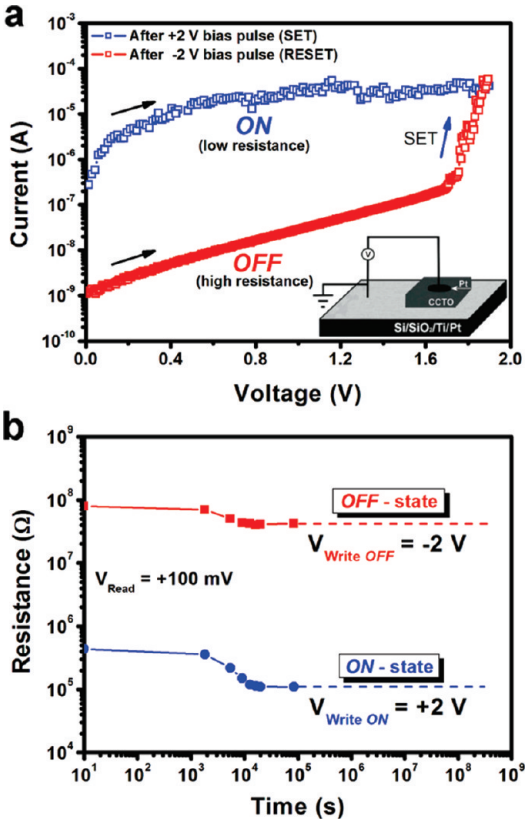

Figure 4. (a) Characteristic $I-V$ curve for the microcapacitors based on CCTO-sputtered nanorods. (b) Time-dependent curves of the stored data for the ON and OFF electrical resistance states.

electroforming process necessary for device activation, a positive voltage pulse switches the resistance from the high (OFF) to low (ON) state when its operation point is SET. Similarly, when the device is in the RESET operation point, a negative operation pulse switches back the resistance position from ON to OFF. The SET and RESET operation points are similar to the ReRAM logic writing states "1" (ON) and "0" (OFF). For these states to be stored in the CCTO microcapacitor, potential differences of around 2 V are necessary. As for the reading states, smaller voltage values are needed. In our case, a suitable value was found to be +100 mV.

Figure 4b show the time-dependent curves of the stored data for the ON and OFF electrical resistance states. Prior to this, the device was activated for the ON and OFF states by applying voltages of +2 and −2 V, respectively, as previously commented. A +100 mV bias was used in order to read the electrical resistance values after different time intervals. Both states exhibit good stability, with a small decrease in both resistances after a few hours, but without long-term electrical degradation. This confirms the nonvolatile nature of the device.

3.2. Model for the Resistive-Switching Mechanism. Two models for the resistance-switching phenomenon are more widely accepted by the scientific community. One implies that the electronic transport occurs through charges trapped in the bulk of the material (dopants, vacancies, metallic clusters, nanodomains, etc.), which control the electrical current levels. The second one refers to resistance changes at the metal/semiconductor interface, modifying in this way the Schottky-like barrier width and/or height.[31] We herein present a possible mechanism

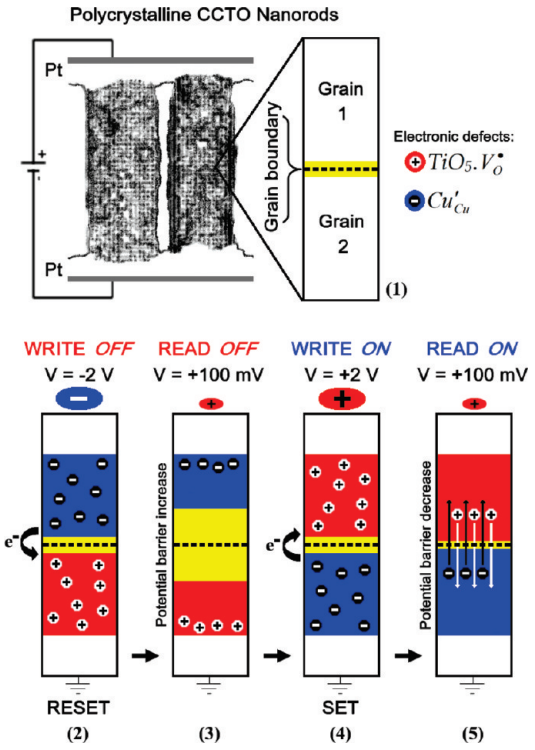

Figure 5. Schematic diagram illustrating the proposed mechanism responsible for switching the resistance of CCTO nanorods. Conduction paths are formed or broken through changes in the polarization state of the potential barriers at the grain boundaries.

accounting for the hysteresis, resistance-switching, and retention behaviors exhibited by the CCTO nanorods. The mechanism is based on the existence of potential nanobarriers at grain boundaries.

The effect of the double Schottky barrier[32−34] investigated in bulk CCTO could be directly related to the resistance changes observed in the material. The barrier is caused by excess charge that is trapped (depletion region) on the two sides of the grain boundary, where the impurities are ionized. Some regions in the interface may have different concentrations of donors where the potential is positive, or clusters of surface charges where the potential is negative, altering the barrier height.[35] The intergranular cluster concentration can be modified by electromigration of electrons and holes from the grain to the grain boundary induced by the electrical field. The charged species in CCTO would be positive $TiO_5 \cdot V_0^{\bullet}$ or negative Cu'_{Cu}, arising from crystalline defects discussed in the work of Bueno and coworkers.[28] Under the effect of a dc electric field, there would be a higher concentration of oxygen vacancies ($TiO_5 \cdot V_0^{\bullet}$) on one side of the interface and ionized copper Cu^{+} (Cu'_{Cu}) on the other side, thus polarizing the grain boundary. This induced polarization would compensate for part of the trapped charges at the interface through charge injection in the depletion layer. The net result would be a lowering of the potential barriers and an increase in the tunneling current with enhanced ohmic character at the contacts. A similar electromigration process involving oxygen vacancies forming conduction channels and causing changes in the barrier at the electrode interface was discussed by Yang et al.[22] but without effects at grain boundaries as stated in this work.

The proposed mechanism for the significant change in the resistance observed in CCTO nanorods is illustrated in Figure 5 for one grain boundary. Starting from an unpolarized state (1), after the electroforming process, a negative pulse ($V_{\text{write OFF}} = -2$ V) is applied, polarizing the barrier by accumulation of $TiO_5 \cdot V_0^{\bullet}$ and Cu'_{Cu} species. In this state (2), the leakage current is high and the interface acquires a rectifying character. A low positive voltage ($V_{\text{read}} = +100$ mV) applied to the interface with inverted polarization increases the depletion layer, restoring the potential barrier. In this situation (3), the current crossing the nanorod is lower and the system assumes a high resistance state (OFF state). A stronger positive pulse ($V_{\text{write ON}} = +2$ V) is needed in order to invert the polarity of the barrier by electromigration. In this state (4), the compliance level is reached, limiting the maximum current and avoiding a breakdown. In the other reading state (5), applying a low positive voltage ($V_{\text{read}} = +100$ mV) in the same direction as the barrier polarization, the current is high. Electron transfer between $TiO_5 \cdot V_0^{\bullet}$ and Cu'_{Cu} species characterizes the low resistance (ON state) of the material in this situation.

By exploitation of the two stable resistance natures of polycrystalline CCTO nanorods, logic "1" (ON) and "0" (OFF) states can be achieved by application of low writing and erasing voltages (+2 and −2 V, respectively). Resistance switching in 1D nanostructures should be, at least in principle, more reproducible than that in thin films because the conduction pathways are restricted by the morphology of the sample (the only possible current path is along the axis of the rod).

4. CONCLUSIONS

The resistance-switching phenomenon was observed in CCTO nanorods grown by RF sputtering. The peculiar characteristics of these polycrystalline nanostructures yield a strong nonlinear $I-V$ behavior. The $I-V$ results recorded on microcapacitors formed from CCTO nanorods demonstrate that two stable resistance states can be achieved, depending on the polarity and magnitude of the applied potential. Both high and low resistance states are stable for long periods, characterizing a nonvolatile memory behavior. Low writing and erasing voltages, large difference between the "ON" and "OFF" resistance values, nondestructive reading, and good retention are characteristics that make this material a good candidate for resistive memory applications. A qualitative mechanism for resistance-switching properties was proposed involving polarization of defects present at the grain boundaries. This simple model accounts for the experimental observations, with the electrical conduction along the polycrystalline nanorods being strongly influenced by the sign and magnitude of the applied electric fields. Long-term fatigue studies using a suitably large number of switching pulses and a more detailed investigation of the effect of pulse widths are still needed. These studies will be needed during the writing and reading operations in order to qualify these nanostructures for applications in nonvolatile memory devices.

AUTHOR INFORMATION

Corresponding Author

*Fax: 16 3301 6692. E-mail: prbueno@iq.unesp.br.

ACKNOWLEDGMENT

R.T. acknowledges financial support of FAPESP through his doctoral grant (PD 2006/61758-4). All of the authors acknowledge financial support of the FAPESP, CNPq, and CAPES Brazilian

foundations. We also thank Dr. Bostjan Jancar from Advanced Materials Department, Jozef Stefan Institute, Ljubljana, Slovenia, for his help with TEM facilities.

REFERENCES

(1) Homes, C. C.; Vogt, T.; Shapiro, S. M.; Wakimoto, S.; Ramirez, A. P. *Science* **2001**, *293*, 673.
(2) Subramanian, M. A.; Li, D.; Duan, N.; Reisner, B. A.; Sleight, A. W. *J. Solid State Chem.* **2000**, *151*, 323.
(3) Ramirez, A. P.; Subramanian, M. A.; Gardel, M.; Blumberg, G.; Li, D.; Vogt, T.; Shapiro, S. M. *Solid State Commun.* **2000**, *115*, 217.
(4) Chung, S. Y.; Kim, I. D.; Kang, S. J. L. *Nat. Mater.* **2004**, *3*, 774.
(5) Sinclair, D. C.; Adams, T. B.; Morrison, F. D.; West, A. R. *Appl. Phys. Lett.* **2002**, *80*, 2153.
(6) Joanni, E.; Savu, R.; Bueno, P. R.; Longo, E.; Varela, J. A. *Appl. Phys. Lett.* **2008**, *92*, 132110.
(7) Parra, R.; Joanni, E.; Espinosa, J. W. M.; Tararam, R.; Cilense, M.; Bueno, P. R.; Varela, J. A.; Longo, E. *J. Am. Ceram. Soc.* **2008**, *91*, 4162.
(8) Shen, Y. S.; Chiou, B. S.; Ho, C. C. *Thin Solid Films* **2008**, *517*, 1209.
(9) Lo Nigro, R.; Toro, R. G.; Malandrino, G.; Fragala, I. L.; Losurdo, M.; Giangregorio, M. M.; Bruno, G.; Raineri, V.; Fiorenza, P. *J. Phys. Chem. B* **2006**, *110*, 17460.
(10) Chang, L. C.; Lee, D. Y.; Ho, C. C.; Chiou, B. S. *Thin Solid Films* **2007**, *516*, 454.
(11) Deng, G.; Xanthopoulos, N.; Muralt, P. *Appl. Phys. Lett.* **2008**, *92*, 172909.
(12) Prakash, B. S.; Varma, K. B. R.; Michau, D.; Maglione, M. *Thin Solid Films* **2008**, *516*, 2874.
(13) Wang, N.; Cai, Y.; Zhang, R. Q. *Mater. Sci. Eng., R* **2008**, *60*, 1.
(14) Xia, Y. N.; Yang, P. D.; Sun, Y. G.; Wu, Y. Y.; Mayers, B.; Gates, B.; Yin, Y. D.; Kim, F.; Yan, Y. Q. *Adv. Mater.* **2003**, *15*, 353.
(15) Joanni, E.; Savu, R.; Jancar, B.; Bueno, P. R.; Varela, J. A. *J. Am. Ceram. Soc.* **2010**, *93*, 51.
(16) Lin, C. C.; Lin, C. Y.; Lin, M. H.; Lin, C. H.; Tseng, T. Y. *IEEE Trans. Electron Devices* **2007**, *54*, 3146.
(17) Guan, W. H.; Long, S. B.; Liu, Q.; Liu, M.; Wang, W. *IEEE Electron Device Lett.* **2008**, *29*, 434.
(18) Schroeder, H.; Jeong, D. S. *Microelectron. Eng.* **2007**, *84*, 1982.
(19) Park, J. W.; Park, J. W.; Kim, D. Y.; Lee, J. K. *J. Vac. Sci. Technol., A* **2005**, *23*, 1309.
(20) Waser, R. *Microelectron. Eng.* **2009**, *86*, 1925.
(21) Shi, J. P.; Zhao, Y. G.; Zhang, H. J.; Tian, H. F.; Zhang, X. P. *Appl. Phys. Lett.* **2009**, *94*, 192103.
(22) Yang, J. J.; Pickett, M. D.; Li, X. M.; Ohlberg, D. A. A.; Stewart, D. R.; Williams, R. S. *Nat. Nanotechnol.* **2008**, *3*, 429.
(23) Szot, K.; Speier, W.; Bihlmayer, G.; Waser, R. *Nat. Mater.* **2006**, *5*, 312.
(24) Choi, B. J.; Jeong, D. S.; Kim, S. K.; Rohde, C.; Choi, S.; Oh, J. H.; Kim, H. J.; Hwang, C. S.; Szot, K.; Waser, R.; Reichenberg, B.; Tiedke, S. *J. Appl. Phys.* **2005**, *98*, 033715.
(25) Seo, S.; Lee, M. J.; Seo, D. H.; Jeoung, E. J.; Suh, D. S.; Joung, Y. S.; Yoo, I. K.; Hwang, I. R.; Kim, S. H.; Byun, I. S.; Kim, J. S.; Choi, J. S.; Park, B. H. *Appl. Phys. Lett.* **2004**, *85*, 5655.
(26) Sawa, A.; Fujii, T.; Kawasaki, M.; Tokura, Y. *Appl. Phys. Lett.* **2004**, *85*, 4073.
(27) Baikalov, A.; Wang, Y. Q.; Shen, B.; Lorenz, B.; Tsui, S.; Sun, Y. Y.; Xue, Y. Y.; Chu, C. W. *Appl. Phys. Lett.* **2003**, *83*, 957.
(28) Bueno, P. R.; Tararam, R.; Parra, R.; Joanni, E.; Ramirez, M. A.; Ribeiro, W. C.; Longo, E.; Varela, J. A. *J. Phys. D: Appl. Phys.* **2009**, *42*, 055404.
(29) Cordeiro, M. A. L.; Souza, F. L.; Leite, E. R.; Lanfredi, A. J. C. *Appl. Phys. Lett.* **2008**, *93*, 182912.
(30) Hwang, I.; Choi, J.; Hong, S.; Kim, J. S.; Byun, I. S.; Bahng, J. H.; Koo, J. Y.; Kang, S. O.; Park, B. H. *Appl. Phys. Lett.* **2010**, *96*, 053112.
(31) Rozenberg, M. J.; Inoue, I. H.; Sanchez, M. J. *Phys. Rev. Lett.* **2004**, *92*, 178302.
(32) Marques, V. P. B.; Bueno, P. R.; Simoes, A. Z.; Cilense, M.; Varela, J. A.; Longo, E.; Leite, E. R. *Solid State Commun.* **2006**, *138*, 1.
(33) Kim, I. D.; Rothschild, A.; Tuller, H. L. *Appl. Phys. Lett.* **2006**, *88*, 072902.
(34) Zang, G. Z.; Zhang, J. L.; Zheng, P.; Wang, J. F.; Wang, C. L. *J. Phys. D: Appl. Phys.* **2005**, *38*, 1824.
(35) Mahan, G. D. *J. Appl. Phys.* **1984**, *55*, 980.